Journal of Engineering Excellence
ISSN: **3108-2793** | Volume 2 Issue 2 April-June 2026
www.jeejournal.com **JEE-08**

AN ADVANCED COST-OPTIMIZED SOLAR MOTOR DRIVE WITH LIMITED SENSOR INTEGRATION

[#1]**Gogu Vamshikrishna,** *Department of EEE,*
[#2]**Mr.N.Kiran Kumar,** *Associate Professor, Department of EEE,*
Vaageswari College of Engineering(Autonomous), Karimnagar, TG.

ABSTRACT: The cost-optimized solar motor propulsion system in this paper is distinguished by its increased efficiency and dependability, which are achieved with minimal sensor integration. The proposed architecture employs intelligent control algorithms and minimal hardware requirements to maintain efficient performance in a diverse array of solar irradiance scenarios, all while reducing overall system costs. The system's complexity, robustness, and maintenance requirements are all reduced by employing fewer sensors and use of estimate approaches. The drive is intended for applications that prioritize cost-effectiveness and long-term reliability, such as agricultural pumps and remote power systems. The proposed method surpasses conventional sensor-rich solar drive systems in terms of motor stability, energy efficiency, and cost reductions, as evidenced by both experimental and simulation data.

Keywords: *Solar motor drive, Cost optimization, Limited sensor integration, Sensorless control, Photovoltaic systems, Energy efficiency, Intelligent control,*

I. INTRODUCTION

The primary goal of our research is to create a solar motor drive system that is both more cost-effective and necessitates fewer sensors, in order to address the growing demand for renewable energy alternatives that are both efficient and affordable. Solar-powered motor systems are gaining popularity for a variety of applications, such as agricultural irrigation, water pumping, and electrifying rural areas, due to their environmental friendliness and lack of dependence on conventional power lines. However, the complexity of the design and the high initial costs of these systems, which are primarily the result of the abundance of sensors and related hardware components, prevent their widespread use.

In order to ensure precise control and consistent operation, conventional solar motor drive systems employ a variety of sensors to monitor variables such as location, speed, voltage, and current. These sensors improve system performance; however, they also increase prices, complicate system design, and result in decreased reliability due to sensor failures. The recent focus of research has been on strict sensor or sensorless control techniques, which predict essential system characteristics using sophisticated algorithms rather than actively monitoring them in order to resolve these issues.

II. LITERATURE SURVEY

R. Sharma 2025: This research investigates the development of a cost-effective solar

DOI: https://doi.org/10.5281/zenodo.20637106

motor drive system that incorporates minimal sensors to minimize hardware complexity while maintaining optimal performance. The research was conducted using estimate methods and sensorless control techniques, rather than a multitude of tangible sensors. The results indicate that system dependability, maintenance requirements, and motor efficiency are all improved under varying conditions of solar irradiation.

P. Kumar 2024: This research, which concentrates on adaptive control systems and observers, investigates advanced control strategies for solar motor actuators that minimize the dependence on sensors. The paper demonstrates that the long-term savings would be substantial if real-time torque and speed estimation could supplant conventional sensors. The results clearly demonstrate enhanced reliability and performance in applications such as rural electricity generation and water irrigation.

S. Ahmed 2023: This research concentrates on the integration of intelligent algorithms into solar-powered motor drive systems in order to enhance energy efficiency with a limited number of sensors. Two methods are employed to improve dynamic responsiveness: artificial intelligence-based estimators and model predictive control (MPC). The paper also reveals that the system is more resilient to shifting climatic conditions and that power losses are reduced.

Dr. V. Meenakshi 2022: The installation of inexpensive solar motor drivers is impeded by two obstacles: control stability without extensive sensing and accurate parameter estimation. In order to resolve these concerns, the investigation implements sliding mode control and imprecise logic. The results indicate increased dependability, improved control accuracy, and a reduced reliance on expensive sensor equipment.

A. Das 2021: This investigation investigates the advantages and disadvantages of solar motor drive systems that optimize cost while incorporating sensors in a minimal manner. Despite the advantages that have been identified, including reduced system costs, simplified designs, and increased durability, control complexity and estimating accuracy remain challenges. The paper's results underscore the necessity of sophisticated estimating methods and hybrid control strategies to enhance system performance and create more sustainable energy solutions.

III. DESIGN OF PROPOSED SYSTEM

Figure 1 illustrates the PV water extraction system's configuration. A boost converter is implemented subsequent to a solar array. The pump and motor are supplied with pulse width modulated power by a VSI. In order to optimize the quantity of accessible radiation, an incremental conductance technique is employed to regulate the power of a PV array. IMD is provided with a reference speed by the V/f controller.

DOI: https://doi.org/10.5281/zenodo.20637106

Journal of Engineering Excellence
ISSN: **3108-2793** | Volume 2 Issue 2 April-June 2026
www.jeejournal.com **JEE-08**

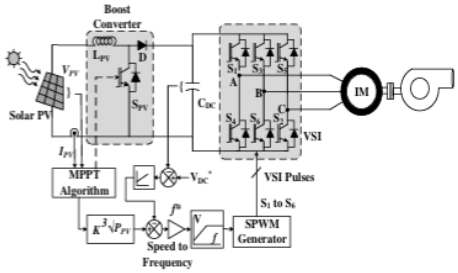

Fig1. System architechure for the standalone solar water pumping system

Design of Solar PV Array

The proposed installation utilizes a 2.2 kW induction motor. The PV array's capacity should be equivalent to that of the motor, provided that there are no losses in the motor or compressor. In this case, a 2.4 kW photovoltaic array is chosen.

$$P_{mp} = \left(N_p \times I_{mp}\right) \times \left(N_s \times V_{mp}\right) = 2.4\ \text{kW}$$

IMP is the current at MPP, Vmp is the voltage of the PV panels at MPP, and Pmp is the utmost power that panels can extract under a specific radiation condition. The number of modules linked in series is denoted by Ns, while the number of modules linked in parallel is denoted by Np. The panel consumes 2.4 kW of power and has an open circuit voltage that is nearly equivalent to a DC link voltage. There are 11 modules in series and 1 in parallel. You can determine the modules and arrays that are necessary to utilize them by consulting Table I.

Table1: Specifications of the Solar Module And Array

Module peak power of the single module	225 W
Module open circuit voltage (v_{oc})	41.79 V
Module short circuit current (i_{sc})	7.13 A
Module voltage at MPP (v_{mp})	33.9 V
Module current at MPP (i_{mp})	6.63 A
Array peak power (P_{mp})	2.4 kW
Array open circuit voltage (V_{oc})	459.69
Array short circuit current (I_{sc})	7.13 A
Array voltage at MPP (V_{mp})	372.9 V
Array current at MPP (I_{mp})	6.63 A

Selection of DC Link Voltage

A formula is employed to determine the DC transit voltage at VSI.

$$m \times \frac{V_{DC}}{2\sqrt{2}} = \frac{V_{L-L}}{\sqrt{3}}$$

The modulation index (m) and the line voltage (VL-L) between the motor terminals are established. Therefore, given that

$$V_{DC} = \frac{2\sqrt{2}}{\sqrt{3}} \times 230 = 375V\ ,$$

When the modulation index is 1, the DC link voltage is 400 V.

Design of DC Link Capacitor

The DC link capacitor is designed to provide an adequate amount of energy during transients, including significant load spikes and radiation reduction. The method for estimating its value is as follows:

$$\frac{1}{2} C_{DC} [V^{*2}_{DC} - V^{2}_{DC1}] = 3\alpha VIt$$

$$\frac{1}{2} C_{DC} [400^2 - 375^2] = 3 \times 1.2 \times 133 \times 8.2 \times 0.005$$

$$C_{DC} = 2026\ \mu\text{F}$$

The set DC bus voltage is denoted by VDC* in the previous calculation, while VDC1 is a suitable lesser value for transients. Furthermore, the transient duration is denoted by t, while α is an overloading factor.

Selection of DC-DC Boost Converter

D is the duty cycle of the booster inductor, which is represented as this:

$$D = \frac{V_{DC} - V_{mp}}{V_{DC}} = \frac{400 - 373}{400} = 0.0675$$

$$L_m = \frac{V_{mp} D}{\Delta I_1 f_s} = \frac{372.9 \times 0.0677}{(0.2 \times 7.6 \times 10000)} = 1.875\ mH$$

DOI: https://doi.org/10.5281/zenodo.20637106

Journal of Engineering Excellence
ISSN: **3108-2793** | Volume 2 Issue 2 April-June 2026
www.jeejournal.com **JEE-08**

The inductance L value of 3 mH is designated when the switching frequency (fs) and ripple current (ΔI1) are taken into account.

Design of Pump

The proportionality constant (Kpump) of a particular water pump is as follows:

$$K_{pump} = \frac{T_L}{\omega_r^2}$$

where TL represents the load torque of the water pump and ϋr is the rotor's rotating speed in rad/sec. This would be the torque output of a steady-state induction motor. Given the induction motor's rated torque of 14.69 N-m and its speed of 1430 rpm. Subsequently, the proportionality constant (Kpump) is approximated as (utilizing equation (6)).

$$K_{pump} = \frac{14.69}{(2*\pi*1430/60)^2} = 6.55\times 1$$

Consequently, the equality constant is selected to be 6.55*10-4 Nm/(r/s).

IV. RESULTS AND DISCUSSION

Utilizing the simulation program, a two-stage PV-fed water pumping system is evaluated. The MATLAB/Simulink environment is used to develop, model, and evaluate the proposed system. By simulating a sudden increase or decrease in solar radiation, the system's efficacy in dynamic conditions is evaluated.

Starting Performance of Proposed System

Figure 4 illustrates numerous attributes of the proposed water pumping system when exposed to 500 W/m2 radiation. The DC link of the VSI is activated during initialization. The VSI DC connection is used to measure the open circuit voltage of the PV array, as the switching device of the boost converter is disabled. The instant the motor speed increases, it begins to decelerate. The current flowing through the PV array reaches Imp as it increases from zero. When the MPPT control of the boost converter is activated and the frequency approaches a threshold, the PV voltage reaches Vmp. After activating the boost converter, the system attains the required MPP at t = 8 s. The DC link voltage eventually stabilizes at the reference value when the PI controller is activated. The sluggish start is evident in the graphic, as the motor current remains below the rated current. The motor's lifespan is extended by this procedure.

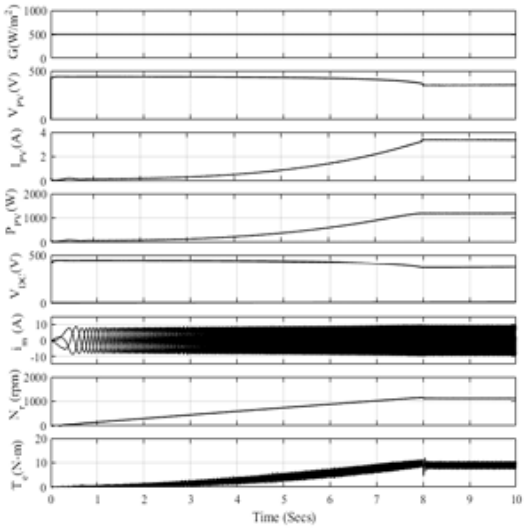

Fig.4. Starting performance of the proposed system

B. Steady State and Dynamic Performances of Proposed System

Figure 5 illustrates the autonomous PV water flow system that has been proposed.

DOI: https://doi.org/10.5281/zenodo.20637106

Diverse degrees of solar radiation are illustrated in this diagram. Between 1 s and 2 s, the solar insolation is 800 W/m2. The accompanying MPP contains the PV indices. We can evaluate the effectiveness of the MPPT method by simulating a decrease in solar insolation at t = 2 s. Despite the fact that the photovoltaic (PV) current fluctuates in accordance with the available insolation, the PV voltage remains stable. Furthermore, the DC bus voltage consistently maintains the 400 V reference value. The motor's speed and torque decrease in direct proportion to the PV power. This continues until the solar insolation slope of the system increases, which occurs at t = 4 s. The PV voltage remains remarkably consistent, as it has in the past; however, the PV current begins to increase as a consequence of solar radiation. Consequently, the motor's speed and torque are directly proportional to the quantity of power that can be extracted from the PV source. At t = 6 s, the system achieves a constant state operation with 1000 W/m2 of solar energy. The system experiences a step decline in solar insolation from 1000 W/m2 to 500 W/m2, resulting in an abrupt decrease in PV current at t = 7 s. The PV voltage continues to exhibit a minimal number of transients. The reference voltage is rapidly reestablished following brief fluctuations in the DC bus voltage. It is crucial to note that the DC bus voltage is not impacted by a 50% reduction in rated power. At t = 9 s, there is a substantial increase in solar insolation. The DC bus voltage remains constant, in accordance with the system's history, while the PV voltage fluctuates minimally. For the power to be balanced, the speed and torque of a motor must increase in direct proportion to the power supplied by the source.

V. CONCLUSION

Ultimately, a cost-optimized solar motor drive that integrates sensors minimally is a highly developed, economically feasible alternative for renewable energy motor applications. The system's performance is not compromised, and it accomplishes reduced costs, enhanced reliability, and simplified design by utilizing intelligent control and estimate approaches and eliminating reliance on various sensors. The utilization of efficient power converters and adaptive control methods ensures consistent operation, irrespective of fluctuations in solar and load conditions. This makes the method ideal for widespread implementation, particularly in remote regions where financial resources are scarce, and it promotes the development of economically viable and environmentally favorable technology.

REFERENCES

[1] E. Drury, T. Jenkin, D. Jordan, and R. Margolis, “Photovoltaic investment risk and uncertainty for residential customers,” IEEE J. Photovoltaics, vol. 4, no. 1, pp. 278–284, Jan. 2014.

[2] E. Muljadi, “PV water pumping with a peak-power tracker using a simple six-step square-wave inverter,” IEEE Trans. on Ind. Appl., vol. 33, no. 3, pp. 714-721, May-Jun 1997.

DOI: https://doi.org/10.5281/zenodo.20637106

[3] U. Sharma, S. Kumar and B. Singh, "Solar array fed water pumping system using induction motor drive," 1st IEEE Intern. Conf. on Power Electronics, Intelligent Control and Energy Systems (ICPEICES), Delhi, 2016.

[4] T. Franklin, J. Cerqueira and E. de Santana, "Fuzzy and PI controllers in pumping water system using photovoltaic electric generation," IEEE Trans. Latin America, vol. 12, no. 6, pp. 10491054, Sept. 2014.

[5] R. Kumar and B. Singh, "BLDC Motor-Driven Solar PV Array-Fed Water Pumping System Employing Zeta Converter," IEEE Trans. Ind. Appl., vol. 52, no. 3, pp. 2315-2322, May-June 2016.

[6] S. Jain, A. K. Thopukara, R. Karampuri and V. T. Somasekhar, "A Single-Stage Photovoltaic System for a Dual-Inverter-Fed Open-End Winding Induction Motor Drive for Pumping Applications," IEEE Trans. Power Elect., vol. 30, no. 9, pp. 4809-4818, Sept. 2015.

[7] J. Caracas, G. Farias, L.Teixeira and L. Ribeiro, "Implementation of a High-Efficiency, High-Lifetime, and Low-Cost Converter for an Autonomous Photovoltaic Water Pumping System," IEEE Trans. Ind. Appl., vol. 50, no. 1, pp. 631-641, Jan.-Feb. 2014.

[8] R. Antonello, M. Carraro, A. Costabeber, F. Tinazzi and M. Zigliotto, "Energy-Efficient Autonomous Solar Water-Pumping System for Permanent-Magnet Synchronous Motors," IEEE Trans. Ind. Electron., vol. 64, no. 1, pp. 43-51, Jan. 2017.

[9] M. Calavia1, J. M. Perié1, J. F. Sanz, and J. Sallán, "Comparison of MPPT strategies for solar modules," in Proc. Int. Conf. Renewable Energies Power Quality, Granada, Spain, Mar. 22–25, 2010.

[10] Trishan Esram and Patrick L. Chapman, "Comparison of photovoltaic array maximum power point tracking techniques," IEEE Transactions on Energy Conversion EC, vol. 22, no.2, pp. 439, 2007.

DOI: https://doi.org/10.5281/zenodo.20637106